

Supporting Information for “Improved constraints on northern extratropical CO₂ fluxes obtained by combining surface-based and space-based atmospheric CO₂ measurements”

B. Byrne¹, J. Liu², M. Lee², I. Baker³, K. W. Bowman², N. M. Deutscher⁴,

D. G. Feist⁵, D. W. T. Griffith⁴, L. T. Iraci⁶, M. Kiel², J. S. Kimball⁷,

C. E. Miller², I. Morino⁸, N. C. Parazoo², C. Petri⁹, C. M. Roehl¹⁰,

M. K. Sha¹¹, K. Strong¹², V. A. Velazco⁴, P. O. Wennberg^{10,13}, D. Wunch¹²

¹NASA Postdoctoral Program Fellow, Jet Propulsion Laboratory, California Institute of Technology, CA, USA

²Jet Propulsion Laboratory, California Institute of Technology, CA, USA

³Atmospheric Science Department, Colorado State University, Fort Collins, CO, USA

⁴Centre for Atmospheric Chemistry, University of Wollongong, Wollongong, Australia

⁵Max Planck Institute for Biogeochemistry, Jena, Germany

⁶Atmospheric Science Branch, NASA Ames Research Center, Moffett Field, CA 94035, USA

⁷Numerical Terradynamic Simulation Group, W.A. Franke College of Forestry & Conservation, The University of Montana,

Missoula, MT 59812, USA

⁸Satellite Observation Center, Center for Global Environmental Research, National Institute for Environmental Studies (NIES),

16-2 Onogawa, Tsukuba, Ibaraki 305-8506, Japan

⁹Institute of Environmental Physics, University of Bremen, Bremen, Germany

¹⁰Division of Geological and Planetary Sciences, California Institute of Technology, Pasadena, CA, USA

¹¹Royal Belgian Institute for Space Aeronomy (BIRA-IASB), Brussels, Belgium

¹²Department of Physics, University of Toronto, Toronto, Ontario, Canada

¹³Division of Engineering and Applied Science, California Institute of Technology, Pasadena, CA, USA

©2019. All rights reserved. California Institute of Technology, government sponsorship acknowledged.

Contents of this file

1. Figures S1 to S7

2. Tables S1 to S2

Corresponding author: B. Byrne, Jet Propulsion Laboratory M/S 233-200, 4800 Oak Grove Drive, Pasadena, CA 91109. (brendan.k.byrne@jpl.nasa.gov)



Figure S1. Locations of aircraft observations used in this study for (a) East Asia, (b) North America, and (c) Alaska/Arctic.

Table S1. Mean and standard deviation (std) of data–model mismatch between each flux inversion and aircraft-based CO₂ observations over East Asia, North America, and Alaska/Arctic.

Posterior-simulated-CO₂ was calculated at 4° × 5° spatial resolution.

| Region | | East Asia | | North America | | Alaska/Arctic | |
|-----------------------------|-----------|------------|-----------|---------------|-----------|---------------|-----------|
| data set | prior NEE | mean (ppm) | std (ppm) | mean (ppm) | std (ppm) | mean (ppm) | std (ppm) |
| prior | SiB3 | -0.06 | 0.85 | 0.08 | 0.97 | -0.84 | 1.61 |
| | CASA | -0.01 | 0.76 | 0.26 | 0.56 | -0.59 | 1.36 |
| | FLUXCOM | 1.18 | 0.70 | 1.54 | 0.57 | 1.24 | 1.00 |
| | Mean NEE | 0.37 | 0.57 | 0.63 | 0.54 | -0.06 | 1.16 |
| TCCON | SiB3 | 0.16 | 0.46 | 0.33 | 0.43 | -0.10 | 0.86 |
| | CASA | 0.33 | 0.74 | 0.65 | 0.57 | -0.02 | 1.30 |
| | FLUXCOM | 0.42 | 0.45 | 0.42 | 0.45 | -0.02 | 1.18 |
| | Mean NEE | 0.30 | 0.42 | 0.43 | 0.47 | -0.05 | 1.05 |
| surface-only | SiB3 | 0.01 | 0.44 | 0.34 | 0.35 | -0.06 | 0.80 |
| | CASA | 0.13 | 0.71 | 0.48 | 0.50 | -0.14 | 1.22 |
| | FLUXCOM | 0.22 | 0.60 | 0.46 | 0.33 | -0.01 | 0.88 |
| | Mean NEE | 0.12 | 0.43 | 0.43 | 0.31 | -0.07 | 0.93 |
| GOSAT-only | SiB3 | 0.25 | 0.41 | 0.49 | 0.37 | -0.06 | 0.76 |
| | CASA | 0.14 | 0.36 | 0.43 | 0.36 | -0.17 | 0.81 |
| | FLUXCOM | 0.23 | 0.44 | 0.50 | 0.33 | 0.03 | 0.89 |
| | Mean NEE | 0.21 | 0.33 | 0.47 | 0.32 | -0.06 | 0.79 |
| GOSAT +surface +TCCON | SiB3 | 0.18 | 0.35 | 0.34 | 0.31 | -0.7 | 0.75 |
| | CASA | 0.15 | 0.39 | 0.42 | 0.36 | -0.03 | 0.89 |
| | FLUXCOM | 0.16 | 0.38 | 0.39 | 0.32 | 0.00 | 0.93 |
| | Mean NEE | 0.16 | 0.31 | 0.38 | 0.32 | -0.03 | 0.84 |

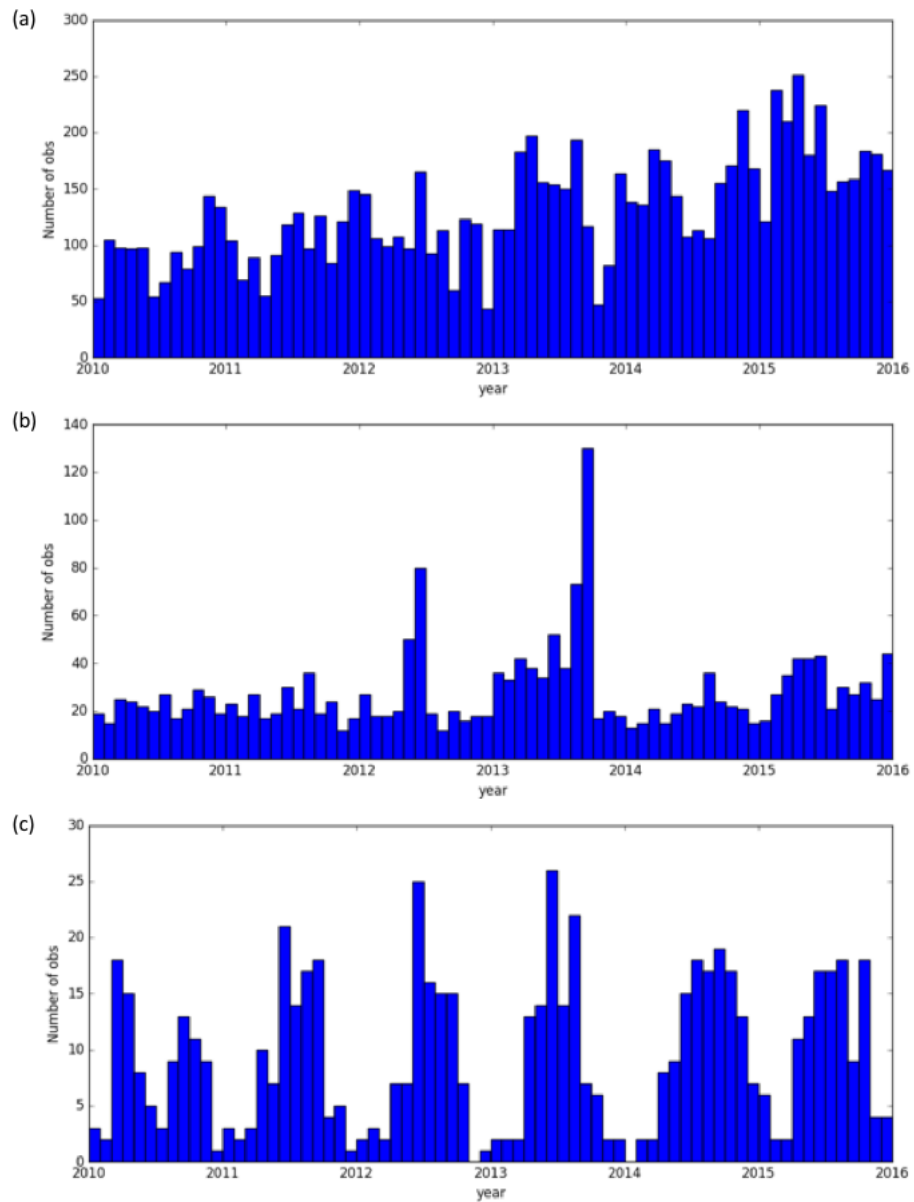


Figure S2. Number of hourly-mean aircraft measurements between 3–8 km altitude above sea level per month for (a) East Asia, (b) North America, and (c) Alaska/Arctic.

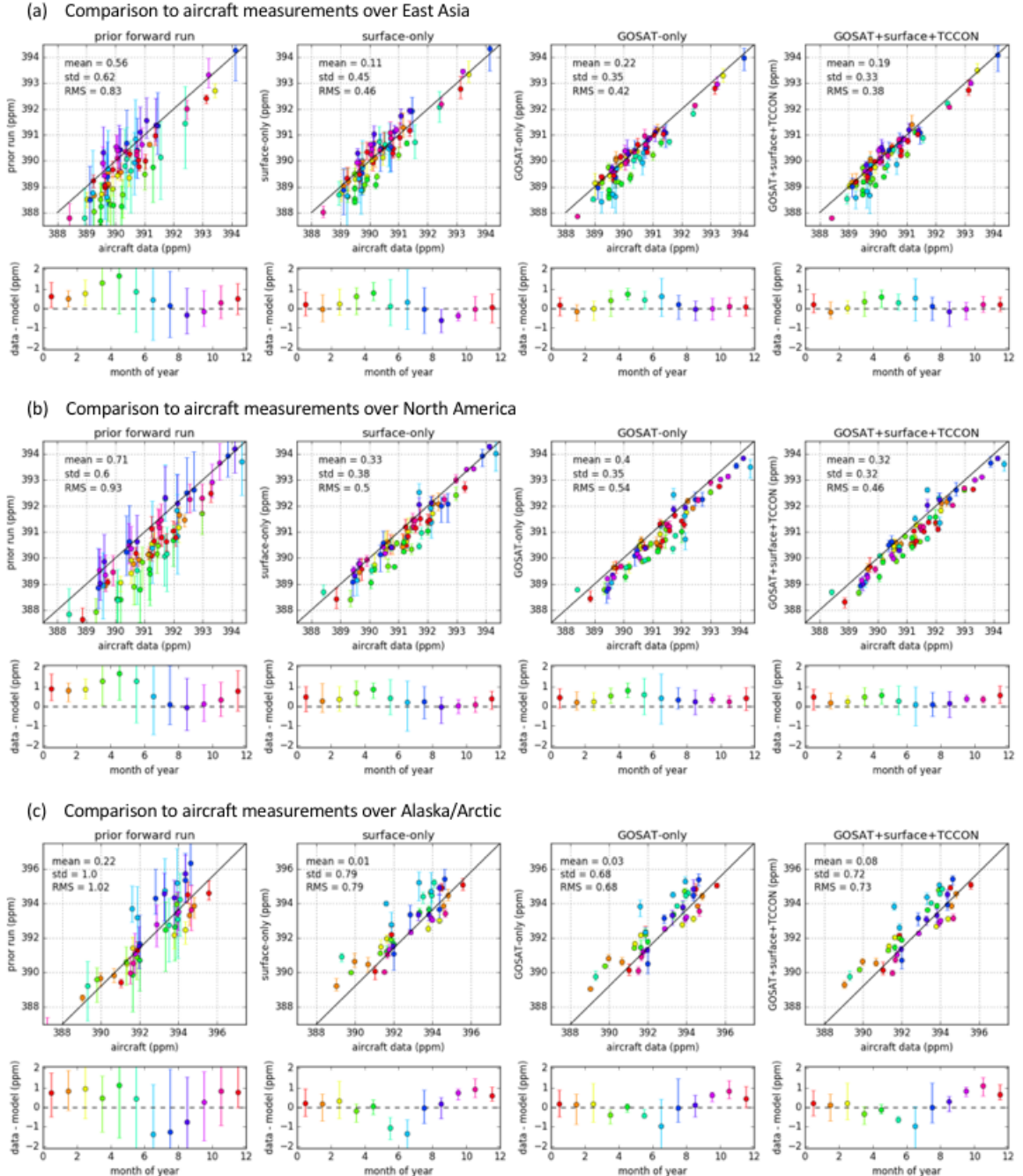


Figure S3. Same as Fig. 3 but at $2^\circ \times 2.5^\circ$ spatial resolution (except for TCCON). Comparison of monthly mean measured and simulated aircraft-based CO₂ for (a) East Asia, (b) North America, and (c) Alaska/Arctic. For each region, the mismatch for (left to right) prior, surface-only, GOSAT-only, and GOSAT+surface+TCCON simulated CO₂ are shown. The top panel shows a scatter plot of the simulated aircraft-based CO₂ against the measured aircraft-based CO₂, and the error bars indicate the spread in posterior NEE. The lower panel shows the mean data–model mismatch for each month, with error bars showing the range of monthly mean mismatched over November 8, 2019, 1:42am

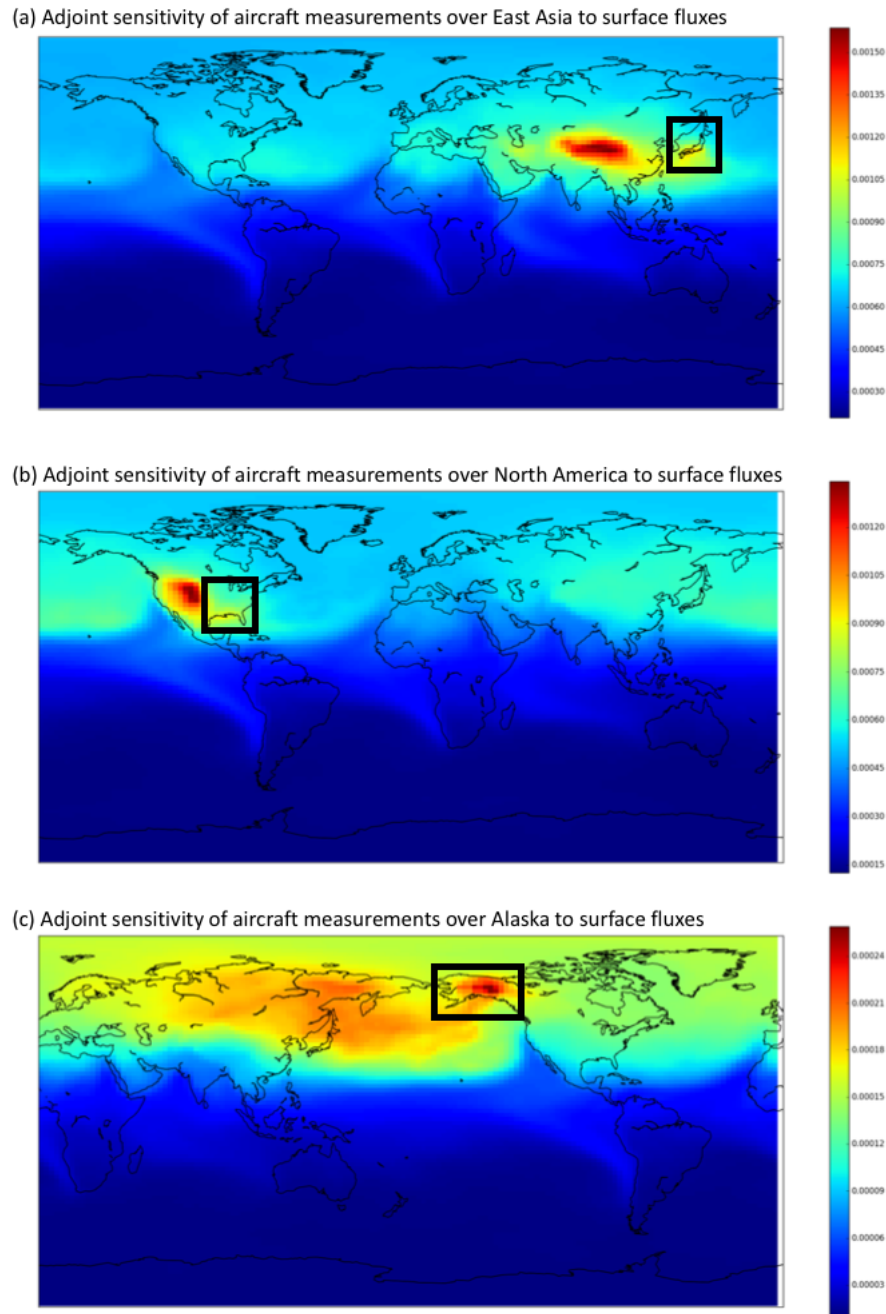


Figure S4. Adjoint sensitivity of aircraft-based CO₂ measurements to surface fluxes for measurements over (a) East Asia, (b) North America, and (c) Alaska/Arctic. Black boxes show the location of aircraft-based CO₂ measurements.

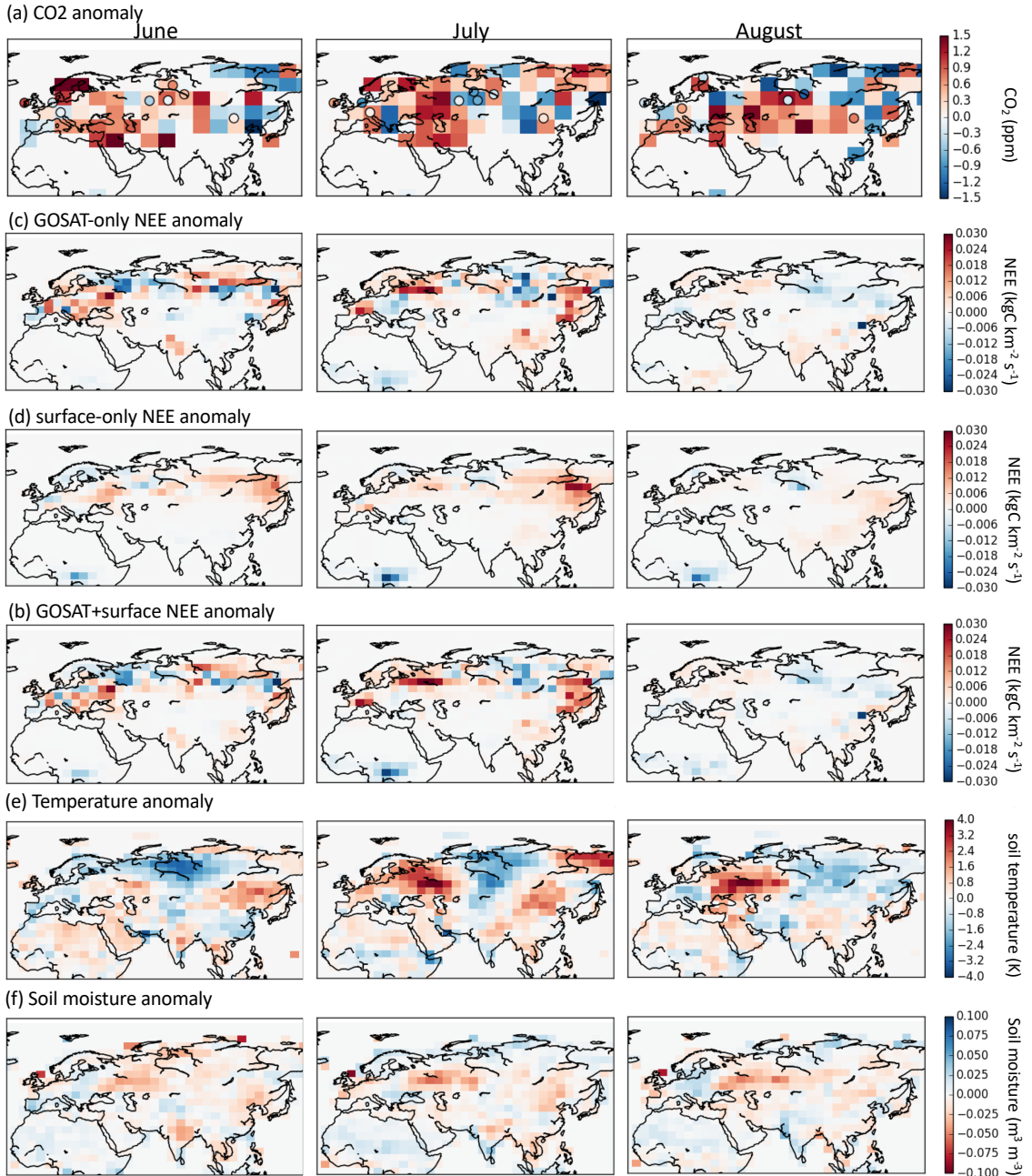


Figure S5. Same as Fig. 8 but for Eurasia during (left-to-right) May, June, July and August of 2010. Monthly anomalies in (a) GOSAT X_{CO₂} (ppm, $4^\circ \times 5^\circ$ grid cells) and surface site CO₂ (ppm divided by four, circles), (b) GOSAT-only posterior NEE, (c) surface-only posterior NEE, (d) GOSAT+surface posterior NEE, (e) MERRA-2 soil temperature anomalies (K), and (f) ESA CCI soil moisture.

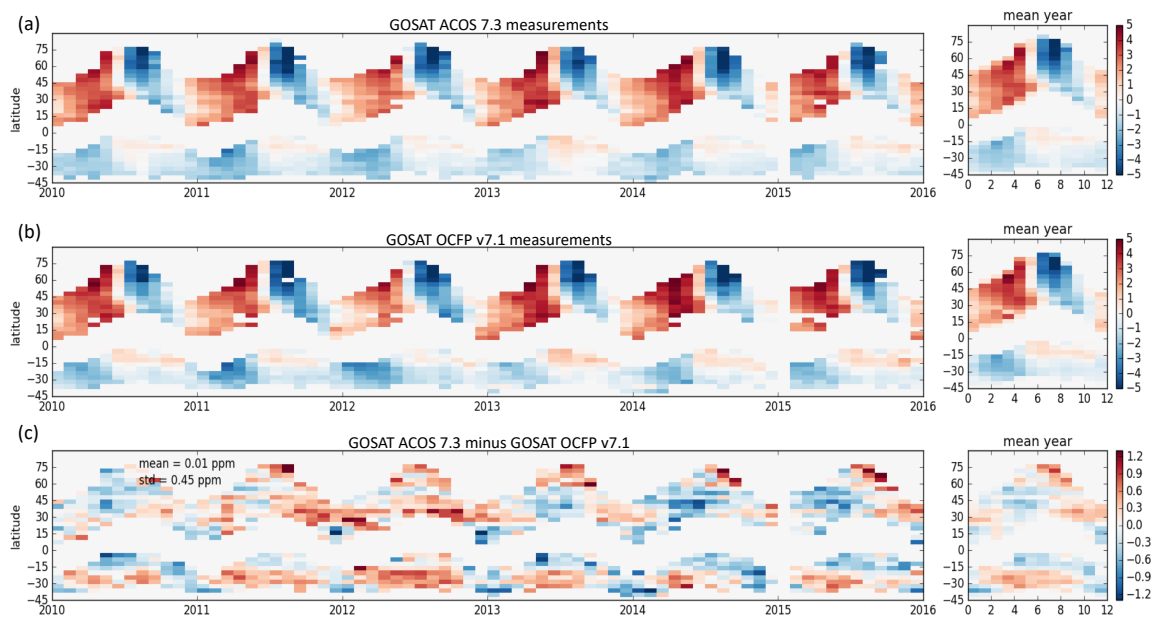


Figure S6. Detrended zonal-monthly mean high-gain nadir GOSAT X_{CO_2} retrieved by (a) ACOS 7.3 and (b) OCFP v7.1. (c) Difference in X_{CO_2} between the two retrieval algorithms.

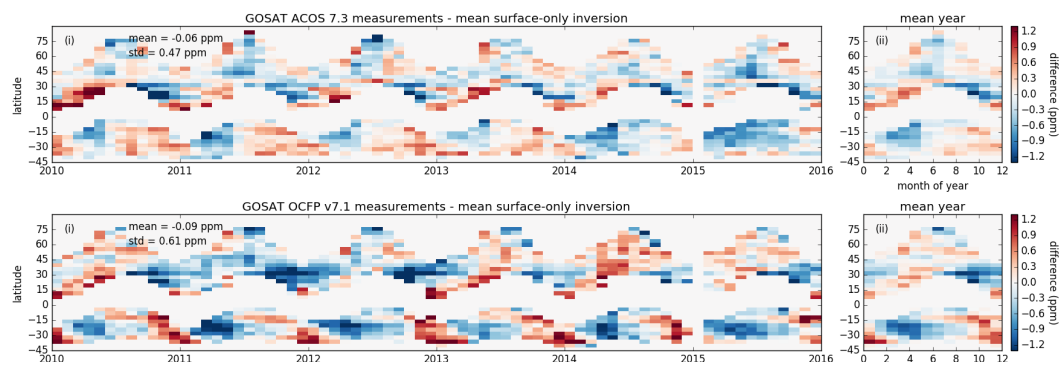


Figure S7. Data-model mismatch of the (a) ACOS 7.3 and (b) OCFP v7.1 GOSAT high-gain nadir X_{CO_2} measurements as a function of latitude and time for the surface-only flux inversion.

Table S2. Mean and standard deviation (std) of data–model mismatch between each flux inversion and aircraft-based CO₂ observations over East Asia, North America, and Alaska/Arctic.

Posterior-simulated-CO₂ was calculated at 2° × 2.5° spatial resolution.

| Region | | East Asia | | North America | | Alaska/Arctic | |
|-----------------------------|-----------|------------|-----------|---------------|-----------|---------------|-----------|
| data set | prior NEE | mean (ppm) | std (ppm) | mean (ppm) | std (ppm) | mean (ppm) | std (ppm) |
| 4prior | SiB3 | 0.57 | 0.94 | 0.56 | 1.03 | 0.01 | 1.56 |
| | CASA | -0.05 | 0.73 | 0.18 | 0.57 | -0.54 | 1.20 |
| | FLUXCOM | 1.16 | 0.75 | 1.39 | 0.62 | 1.19 | 0.90 |
| | Mean NEE | 0.56 | 0.62 | 0.71 | 0.60 | 0.22 | 1.00 |
| surface-only | SiB3 | 0.01 | 0.44 | 0.26 | 0.40 | 0.03 | 0.73 |
| | CASA | 0.11 | 0.69 | 0.38 | 0.57 | -0.06 | 1.04 |
| | FLUXCOM | 0.22 | 0.62 | 0.35 | 0.39 | 0.06 | 0.79 |
| | Mean NEE | 0.11 | 0.45 | 0.33 | 0.38 | 0.01 | 0.79 |
| GOSAT-only | SiB3 | 0.25 | 0.38 | 0.42 | 0.38 | 0.03 | 0.65 |
| | CASA | 0.18 | 0.39 | 0.37 | 0.39 | -0.07 | 0.72 |
| | FLUXCOM | 0.24 | 0.46 | 0.42 | 0.36 | 0.14 | 0.75 |
| | Mean NEE | 0.22 | 0.35 | 0.40 | 0.35 | 0.03 | 0.68 |
| GOSAT +surface +TCCON | SiB3 | 0.20 | 0.37 | 0.28 | 0.33 | 0.06 | 0.66 |
| | CASA | 0.15 | 0.40 | 0.33 | 0.39 | 0.04 | 0.78 |
| | FLUXCOM | 0.22 | 0.38 | 0.36 | 0.32 | 0.15 | 0.78 |
| | Mean NEE | 0.19 | 0.33 | 0.32 | 0.32 | 0.08 | 0.72 |